Structural characterization of an elevated lipid bilayer obtained by stepwise functionalization of a self-assembled alkenyl silane film

Christian Daniel[a)]
Department of Physics, Ludwig-Maximilians-Universität, D-80539 Munich, Germany

Karen E. Sohn[b)] and Thomas E. Mates[c)]
Department of Materials, UCSB, Santa Barbara, California 93106

Edward J. Kramer[d)]
Department of Materials and Department of Chemical Engineering, UCSB, Santa Barbara, California 93106

Joachim O. Rädler,[e)] Erich Sackmann,[f)] Bert Nickel,[g)] and Luisa Andruzzi[h)]
Department of Physics, Ludwig-Maximilians-Universität, D-80539 Munich, Germany

(Received 26 July 2007; accepted 6 September 2007; published 2 October 2007)

This work reports a novel tethered lipid membrane supported on silicon oxide providing an improved model cell membrane. There is an increasing need for robust solid supported fluid model membranes that can be easily deposited on soft cushions. In such architecture the space between the membrane and the substrate should be tunable in the nanometer range. For this purpose a SiO_2 surface was functionalized with poly(ethylene glycol) (PEG)-lipid tethers and further modified with poly(ethylene glycol) making a biologically passivated substrate available for lipid bilayer deposition. First, a short chain self-assembled alkenyl silane film was oxidized to yield terminal COOH groups and then functionalized with amino-terminated PEG-lipids via N-hydroxysuccinimide chemistry. The functionalized silane film was then additionally passivated by functionalization of unreacted COOH groups with amino-terminated PEG of variable chain length. X-ray photoelectron spectroscopy (XPS) analysis of dry films, carried out near the C 1*s* ionization edge to characterize chemical groups formed in the near-surface region, confirmed binding of PEG-lipid tethers to the silane film. XPS further indicated that backfilling with PEG caused the lipid tails to stick up above the PEG layer which was confirmed by the x-ray reflectivity measurements. Lipid vesicle fusion on these surfaces in the presence of excess water resulted in the formation of supported membranes characterized by very high homogeneity and long range mobility, as confirmed by fluorescence bleaching experiments. Even after repeated drying-hydrating cycles, these robust surfaces provided good templates for high fluidity elevated membranes. X-ray reflectivity measurements of the tethered membranes, with a resolution of 0.6 nm in water, showed that these fluid membranes are elevated up to 8 nm above the silicon oxide surface. © *2007 American Vacuum Society.* [DOI: 10.1116/1.2790852]

I. INTRODUCTION

The cell membrane, or "plasma membrane," is the part of any biological cell that encloses the cell. It is a selectively permeable structured bilayer of phospholipid and protein molecules that separates a cell's interior from its surroundings, controlling what moves in and out. The plasma membrane contains receptor proteins, cell adhesion proteins, and other proteins with a variety of functions, such as the regulation of cell behavior and the organization of cells in tissues. The membrane can be envisioned as a quasi-two-dimensional assembly of amphiphilic lipids supported by biopolymer layers (such as the cytoskeleton) and associated with various integral and peripheral proteins. Over the years strategies have been developed to create mechanically and thermally stable cell mimicking surfaces by depositing membranes onto planar solid supports,[1] such as glass,[2] gold,[3] and plastics.[4]

The planar geometry allows for the application of various surface sensitive techniques to characterize the structure and to quantify dynamics of lipid membranes including membrane associated proteins, e.g., annexins.[5] The main drawback of solid supports is that typical distances between the membrane and the substrate range up to 1 nm,[6,7] which is generally not enough to prevent the denaturing of transmembrane proteins.[7] In the effort to space the membrane up from the silicon substrate polymeric cushion materials that can form hydrated thin films such as polyacrylamide,[8] dextran,[9] agarose,[10] polyethyleneimine,[11,12] cellulose derivatives,[13,14]

[a)]Electronic mail: daniel@lmu.de
[b)]Electronic mail: ksohn@mrl.ucsb.edu
[c)]Electronic mail: tmates@mrl.ucsb.edu
[d)]Electronic mail: edkramer@mrl.ucsb.edu
[e)]Electronic mail: joachim.raedler@lmu.de
[f)]Electronic mail: sackmann@lmu.de
[g)]Electronic mail: nickel@lmu.de
[h)]Author to whom correspondence should be addressed; electronic mail: luisa.andruzzi@physik.uni-muenchen.de

and poly(ethylene glycol),[15–17] as well as polyelectrolyte multilayers,[18,19] have been introduced prior to membrane deposition.

An alternative route is to graft amphiphilic polymers (e.g., lipopolymers) directly to the surface and then to use this film as an anchoring platform for a membrane deposited by, e.g., vesicle fusion. The advantages of this strategy are that both the tether density and spacer length can be tuned in such a way that the space underneath the membrane is sufficient to host membrane spanning proteins and, potentially, to adjust the mechanical properties of the membrane.[20] One reported example is the synthesis of a terpolymer having an acrylamide backbone bearing a disulfide moiety for chemisorption onto gold substrates, lipid sidechains for membrane incorporation and amino-terminated triethylene glycol pendent groups as a hydrophilic cushion.[21] A more recent article reported the use of a synthetic thiohexa(ethylene oxide) lipid for chemisorption onto gold surfaces.[22] Another approach uses a tripartite molecule consisting of a lipid attached to a poly(ethylene glycol) molecule with a molecular weight of 3400 Dalton and a silane reactive group for substrate attachment by Langmuir–Blodgett (LB) transfer and thermal annealing.[23]

Similarly, grafting of 2-methyl-2-oxazoline based lipopolymers using LB transfer followed by thermal annealing to induce covalent coupling of the silane to the surface was reported.[24] In a recent work, a tetra(ethylene glycol)-lipid silane has been grafted to an oxide surface without LB transfer.[25] In all cases, tethered bilayer lipid membranes have been successfully accomplished.

In some cases, the functionalization was carried out in two steps, i.e., first a silane based surface modification was employed to provide a reactive group that is functionalized in a second step by the lipopolymer. For example, an oxide surface was first modified by benzophenone and, in a second step, a lipid-containing poly(2-ethyl-2-oxazoline) was grafted to this surface by photocrosslinking.[26] A similar two step strategy has been employed for gold substrates where in a first step a thiopeptide was chemisorbed to a gold surface, and in a second step, its COOH termini were functionalized with DMPE lipids via N-hydroxysuccinimide (NHS) chemistry to form a thiopeptide-tethered lipid monolayer.[27] This strategy is very useful because it involves surface lipid tethering via stable amide bonds.

To date, the approaches to tether lipopolymers to surfaces have indeed proved very useful to create elevated membranes, however, there are still chemical design aspects that can be improved. For example, while sparse tethers are usually desirable to make a membrane fluid, they may not be effective for making the membrane homogeneous due to the low surface tether grafting density, which may also partially expose a bare substrate that will denature biological material. Conversely, too many tethers may cause the resulting elevated membrane to be sparingly fluid and the compact structure of the elevated membrane may impede spanning of proteins through the bilayer. Therefore, a sparsely tethered bilayer resting over a protein resistant biocompatible support such as polyethylene glycol[28,29] (PEG) may provide a yet incremental advancement on previous work on elevated membranes. This type of architecture would also provide a truly biomimetic cell membrane model.

Bearing this in mind, we have developed a stepwise, bottom-up approach that readily provides sparsely tethered lipid films for production of homogeneous and fluid elevated membranes on SiO_2 surfaces. Such an approach combines the use of lipopolymer tethers with a hydrophilic cushioning polymer of variable chain length, making use of the minimum amount of tethers for membrane fluidity while providing passivation of the substrate, which is necessary for the system to behave as a cell-membrane like model. In a three step synthesis, PEG-lipids were covalently bound from low proportion solutions via NHS chemistry to an oxidized self-assembled alkenyl silane film, and the resulting surface was further modified with PEG, in a process denoted hereafter as "backfilling." The functionalization of the SiO_2 surface is performed under mild conditions by creating amide bonds via NHS chemistry, as opposed to top-down approaches where PEG-lipids have been grafted via silanization. The PEG-lipid films were characterized by x-ray photoelectron spectroscopy (XPS) and x-ray reflectivity, and the membrane structure and fluidity were investigated by x-ray reflectivity and fluorescence microscopy based bleaching techniques.

II. EXPERIMENTAL SECTION

A. Materials

Anhydrous hexadecane, anhydrous dimethylformamide (DMF), 1-ethyl-3-[3-(dimethylamino)propyl] carbodiimidehydrochloride (EDC), NHS were purchased from Aldrich and used without further purification. Octenyltrichlorosilane (OCT), 90% vinyl group content, was purchased from ABCR GmbH and used without further purification. Amino-terminated poly(ethyleneglycols) (NH_2-PEG_n, $n=17,45$) were purchased from Nektar and used without further purification. Amino-terminated poly(ethyleneglycol)-functionalized 1,2-distearoyl-*sn*-glycero-3-phosphoethanolamine (DSPE) lipid (NH_2-PEG_{45}DSPE, herein also called PEG-lipid) and 1-stearoyl-2-oleoyl-*sn*-glycero-3-phosphocholine (SOPC) lipid were purchased from Avanti Polar Lipids, Inc. and used without further purification. Lipid fluorescently labeled with nitrobenz-2-oxa-1,3-diazol-4-yl (NBD) was purchased from Molecular Probes. Silicon wafers [100 nm thermally oxidized Si (001), 20×15 mm^2] were purchased from Holm Silicium (Germany).

B. Preparation of octenyltrichlorosilane self-assembled films (1)

Wafers were cleaned in a three step procedure: (i) immersed in a solution of $NH_4OH/H_2O_2/H_2O$ (1/1/4 by volume) at 80 °C for 10 min and washed with de-ionized water, (ii) immersed in a solution of $HCl/H_2O_2/H_2O$ (1/1/4 v/v) at 80 °C for 10 min and washed with de-ionized water, and (iii) immersed in a solution of $NH_4OH/H_2O_2/H_2O$ (1/1/4 v/v) at

80 °C for 10 min and thoroughly washed with de-ionized water. Then, the wafer pieces were flushed with nitrogen and dried in a vacuum oven at 120 °C for 5 min and used within half an hour of cleaning. OCT self-assembled monolayers were prepared according to procedures described in the literature.[30] In a typical reaction, a flask was charged with three silicon wafers, anhydrous hexadecane (15 mL) and octenyltrichlorosilane (0.1 % wt). The mixture was allowed to react under nitrogen for 24 h. After silanization the wafers were rinsed with anhydrous toluene and sonicated in $CHCl_3$ for a few minutes to remove organic residuals. Finally, they were blown dry in nitrogen flow and stored at room temperature under vacuum until usage.

C. Oxidation of OCT film (2)

The OCT film was modified to the corresponding COOH termination via a permanganate-periodate oxidation process.[31] Stock solutions of $KMnO_4$ (5 mM), $NaIO_4$ (195 mM), and K_2CO_3 (18 mM) were prepared. Then, immediately prior to the oxidation, 1 mL from each solution was combined with distilled water to make the oxidizing solution at pH=7.5 and tenfold diluted with respect to each component. The OCT monolayers were exposed to this solution for 24 h to ensure quantitative oxidation of the surface vinyl groups. Then, the samples were rinsed in sequence in 20 mL of $NaHSO_3$ (0.3 mM), water, HCl (0.1 M), water, and ethanol. The samples were finally dried in a flow of nitrogen and stored under vacuum until use.

D. Preparation of PEG-lipid surface (4)

The oxidized OCT wafers were reacted with a water solution of 75 mM EDC and 15 mM NHS for 1 h. Then, they were thoroughly rinsed with water and exposed to a solution of NH_2-PEG$_n$DSPE (1 mg/mL) in anhydrous DMF. The reaction was run overnight, and then wafers were sonicated in $CHCl_3$ for a few minutes and dried under nitrogen flow. Samples were finally dried in a vacuum oven at room temperature for several hours.

E. Preparation of mixed PEG-lipid/PEG surfaces [(5), (6)]

The OCT-PEG-DSPE wafers were reacted with NHS as described before and then exposed to a solution of NH_2-PEG$_n$ (10 mg/mL) in carbonate buffer at pH=8.5. The reaction was run overnight and then wafers were sonicated in $CHCl_3$ for a few minutes and dried under nitrogen flow. Samples were finally dried under vacuum at room temperature for several hours and stored under vacuum until use.

F. Preparation of lipid vesicles

SOPC lipids were prepared according to general procedures described by the manufacturer (Avanti Polar Lipids, Inc.). Lipids were dissolved in chloroform and stored at −20 °C. Lipids were dried to a thin film under a stream of nitrogen gas in a glass vial. The resulting films were placed under vacuum for several hours to remove residual organic solvent. Dried lipids were hydrated in water to a final concentration of 1 mg/mL. Then, the multilamellar vesicle suspension was extruded several times through two stacked 0.1 μm nucleopore polycarbonate filters (Whatman, Clifton, NJ) using a high pressure 10 mL thermobarrel extruder (Northern Lipids, Vancouver, BC) to obtain uniform 100 nm diameter large unilamellar vesicles (LUV). The LUV suspension was then injected into the plastic chamber containing the wafer and incubated for several hours. Finally, water was gently injected into the chamber to wash off loose vesicles.

G. Characterization

Fluorescence microscopy was carried out on a Zeiss fluorescence microscope equipped with a Hamamatsu Orca cooled charge coupled device camera and an acquisition and image analysis software package (Simple PCI, Compix Inc., Sewickley, PA).

X-ray reflectometry measurements were carried out under ambient conditions and in excess water using a microfluidic device. The setup also provides optical access for a fluorescence microscope; a sketch of the device is shown in the supplemental information[48] and more details on this setup can be found in the literature.[4,32] A beam energy of 19.9 keV was selected using a Si (111) monochromator, and the data were recorded with a fast scintillation detector (Cyberstar, Oxford Instruments). The x-ray reflectometry experiments were carried out at the synchrotron beamline D4 at HASYLAB Hamburg. The reflectivity data were modeled with the Parratt formalism[33] using a layered structure with slabs parallel to the surface. The spatial resolution, $d_{\min}$, of these experiments can be estimated to be $d_{\min}=\pi/q_{\max}=0.63$ nm.[34] Here, $q_{\max}=5$ nm^{-1} is the maximum q value up to which we can measure the reflectivity before it drops below the background level. Consequently, slab sizes of 0.7 nm (superimposed by a Gaussian roughness of 0.25 nm) were used to reconstruct the depth profiles of membrane reflectivity data.

XPS was performed at UCSB on a Kratos axis ultraspectrometer (Kratos Analytical, Manchester, UK) using monochromated Al K_α x rays at 1486 eV at 225 W and low energy electrons for charge compensation. Spectra were collected at 40 and 80 eV pass energy using a hemispherical energy analyzer and a channel width of 0.05 eV.

III. RESULTS AND DISCUSSION

A. Synthesis and XPS characterization of PEG-lipid surfaces

Major requirements for a surface-tethered lipid membrane to work as a cell biomimetic model are biocompatibility of the tethering spacer and a low number of tethers, which can eventually impact membrane fluidity and applicability. This work presents a novel architecture of a surface-tethered lipid membrane separated away from a silicon oxide surface by PEG-lipid tethers where the biocompatibility is further im-

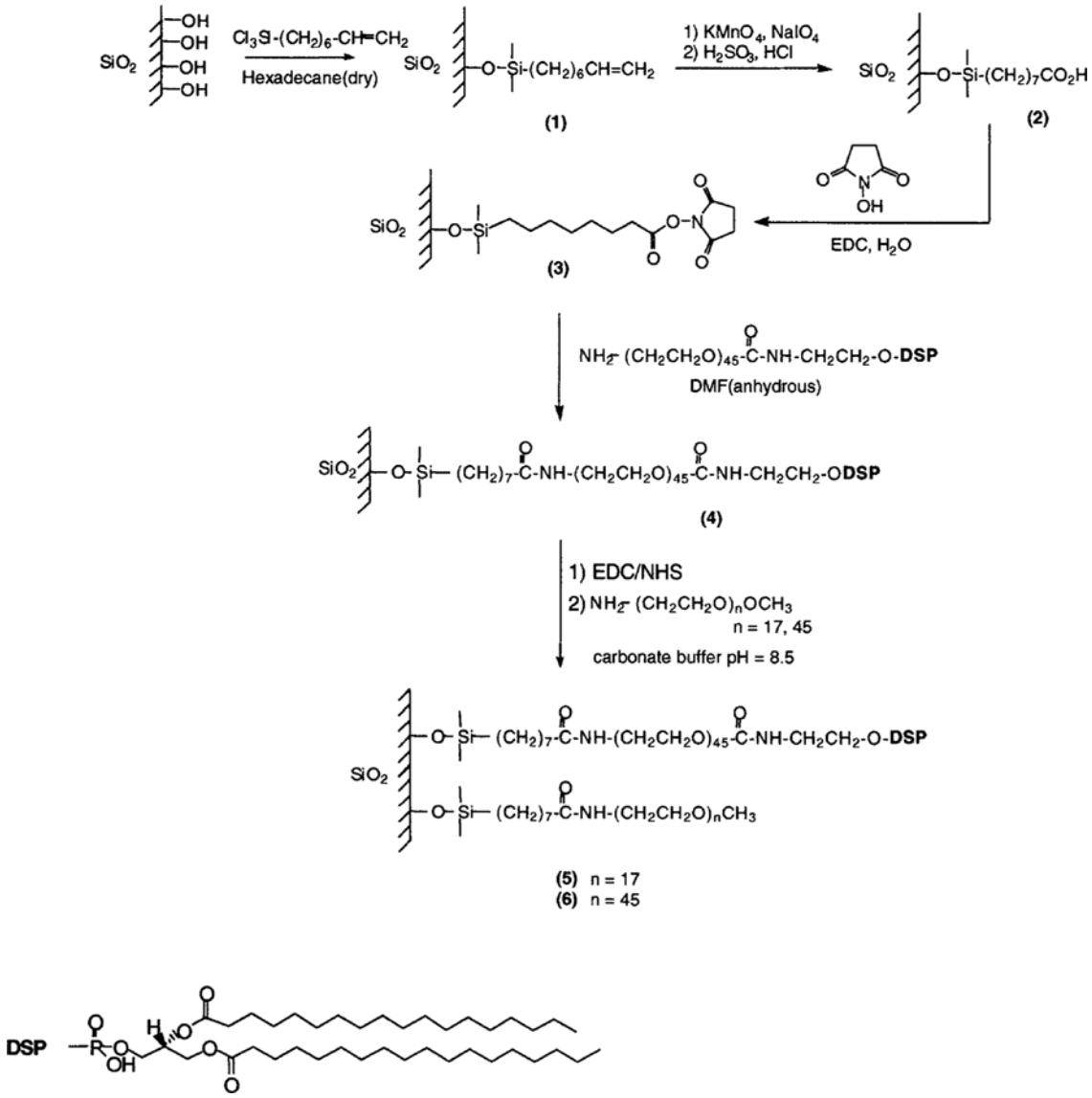

SCHEME 1. Synthesis of PEG-lipid surfaces and mixed PEG-lipid/PEG surfaces where the lipid component is indicated as NH_2-CH_2CH_2-ODSP, i.e., DSPE.

proved by backfilling the substrate with PEG spacers of varying chain length. The synthetic procedure adopted consists of a modular layer-by-layer fabrication as outlined in Scheme 1.

A self-assembled octenyltrichlorosilane film (1) was oxidized by permanganate-periodate reaction converting terminal vinyl groups to COOH functionalities (2). The carboxylated SAM was then reacted with NHS to form active ester groups capable of prompt reaction with amino-terminated molecules forming amide bonds that are stable toward hydrolytic scission. The NHS chemistry has proven to be a useful tool in organic chemistry for producing chemical bonds under mild conditions.[32,33] It allows for the formation of amide and ester bonds between carboxylic and amino or hydroxyl groups even at room temperature in aqueous solution. The NHS modified surface (3) was reacted with an aqueous solution containing a low proportion of amino-terminated PEG_nDSPE tethers (n=45) to yield the PEG_nDSPE functionalized SAM (4). Such reaction conditions were chosen in order to leave unreacted surface COOH groups that could be used for a second NHS reactive step with backfilling PEG. Therefore, sample (4) was further modified by functionalization of residual COOH groups with an aqueous solution containing a high proportion of amino-terminated PEG_n of different chain lengths (n=17 and 45) via NHS chemistry to yield mixed PEG-lipid/PEG surfaces (5) and (6). It should be noted that in this reaction a tenfold excess of amino-terminated PEG_n was used as compared to the reaction with amino-terminated PEG_nDSPE to ensure that the yield of reaction of the backfilling was more thermodynamically favored than the yield of reaction with lipids. Furthermore, the molecular weight of PEG_nDSPE (MW =2790 Dalton) is about twice the one of PEG_n (MW=750 and 2000 Dalton), so this also ensures higher surface reactivity of PEG_n than PEG_nDSPE for entropic reasons leading

TABLE I. XPS binding energies near the carbon ionization edge.

Bond	Binding energy (eV)
C-C	285
C-O-C	286.5
O=C-O	289.2

to introduction of backfilling PEG in sample (4) as shown by emission angle dependent XPS data discussed later in the text.

It should be noted that all surfaces were thoroughly sonicated in chloroform prior to x-ray and fluorescence studies. This treatment ensured both the removal of unbound PEG and cleavage of residual NHS esters, thus allowing us to make the assumption that any nitrogen detected by XPS corresponds to the PEG linking amide bond and any detected PEG is covalently bound to the surface.

Contact angle measurements with water as the wetting liquid were performed to check how the wettability of the surface changed after the various stages of the synthesis. The advancing and receding contact angles of (1) were 90° and 82°, respectively, whereas the advancing and receding contact angles for (2) were 35° and 20°, in agreement with values previously reported in the literature for an oxidized vinyl-terminated self-assembled monolayer.[31] The advancing and receding contact angles for surfaces (4)–(6) were about 47° and 30°, respectively, likely due to the presence of a mixed lipid/PEG surface.

High resolution XPS was carried out at the C 1*s* ionization edge to characterize the chemical groups formed in the near surface region during the different stages of the synthesis process. The different bonding environments for the carbon atoms cause their 1*s* electrons to have different binding energies, which are detectable by XPS. Table I shows the expected binding energies for the relevant carbon bonds.

Figure 1 (top) shows high resolution C 1*s* scans of surfaces (1) and (2). The curves are normalized so that the area under the C1*s* peaks equal 1. Sample (1) shows a peak at 285 eV due to the C-C bonds, whereas sample (2) shows an additional peak at 289 eV due to the COOH groups and a shoulder at 286.4 eV likely due to some by-product secondary alcohol formed during the oxidation reaction. Figure 1 (middle) shows C 1*s* curve fitting for sample (4) where an additional peak can be observed at 286.5 eV due to C-O-C bonds in the PEG chain. Figure 1 (bottom) shows survey scans for surfaces (1), (2), and (4), where it can be noted that a small peak appears at 399 eV in sample (4) due to the nitrogen in the PEG-lipid linking amide bond. This peak is not due to residual NHS because the wafers were thoroughly sonicated in water and then chloroform to remove residual NHS and unbound material. Also, it is well known that NHS esters are very unstable and hydrolyze very rapidly in aqueous solution and upon exposure to air.[35]

The COOH peak constitutes a 3.45% fraction of total C peak (for a 100% vinyl group oxidation it should be 12.5%) indicating that about 30% of the initial vinyl groups were

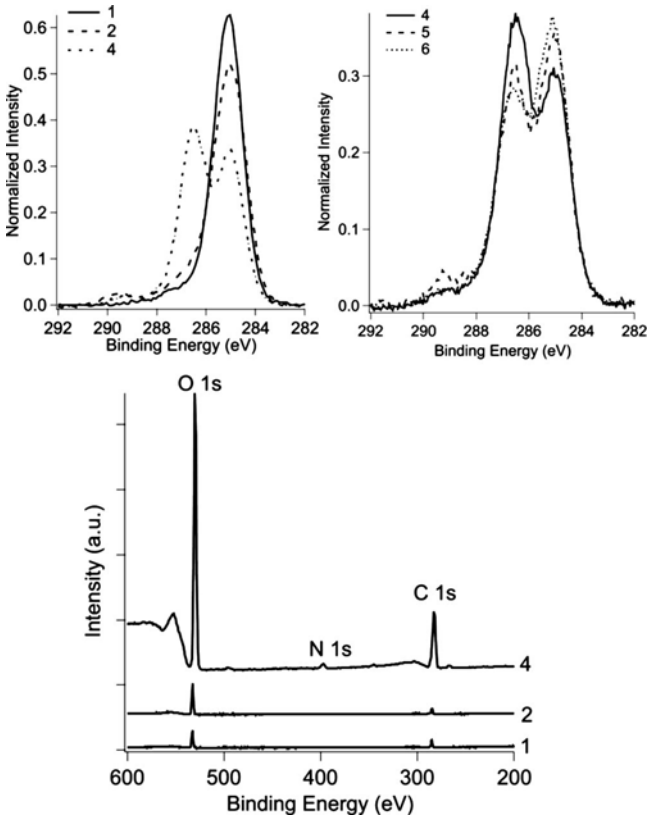

FIG. 1. (Top-left) XPS C 1*s* high resolution scans of samples (1), (2), and (4). (Top-right) XPS C 1*s* high resolution scans of samples (4), (5), and (6). (Bottom) XPS survey scans of samples (1), (2), and (4).

oxidized to COOH groups. Since the ratio between N and unreacted COOH groups at the surface in sample (4) is equal to 1 and the PEGLipid molecule contains two N atoms, it appears that about 30% of the COOH have been functionalized with PEGLipid with the remaining unreacted COOH available for the backfilling reaction. The PEGLipid to PEG ratios in samples (5) and (6) obtained after backfilling could not be calculated based on the N/COOH ratio due to the fact that nitrogen is present in both PEGLipid and PEG. However, the angle dependent XPS data discussed below clearly show introduction of PEG in these samples.

Figure 2 shows high resolution C 1*s* spectra at 0° and 75° emission angles for samples (4), (5), and (6). The two peaks at 285 and 286.5 eV are due to C-C and C-O-C bonds, respectively, as expected from the chemical structure, with the C-C peak being more intense in the near-surface, 75° emission angle spectrum of (4) and (6) due to the lower surface energy aliphatic lipid tails being more exposed at the solid-air interface. It should be noted that the peak intensity ratio (C-C/C-O-C) in sample (4) is lower than in either of the backfilled samples at an emission angle of 0° and that at an emission angle of 75° sample (6), which has the longest backfilled PEG chains ($n=45$, matching the length of PEG in the tethered PEG-lipid), has by far the largest C-C/C-O-C peak intensity ratio. Attaching more long, PEG backfill chains to the SAM may cause the lipid tails to be expelled to the region above the PEG layer. Changes in the electron

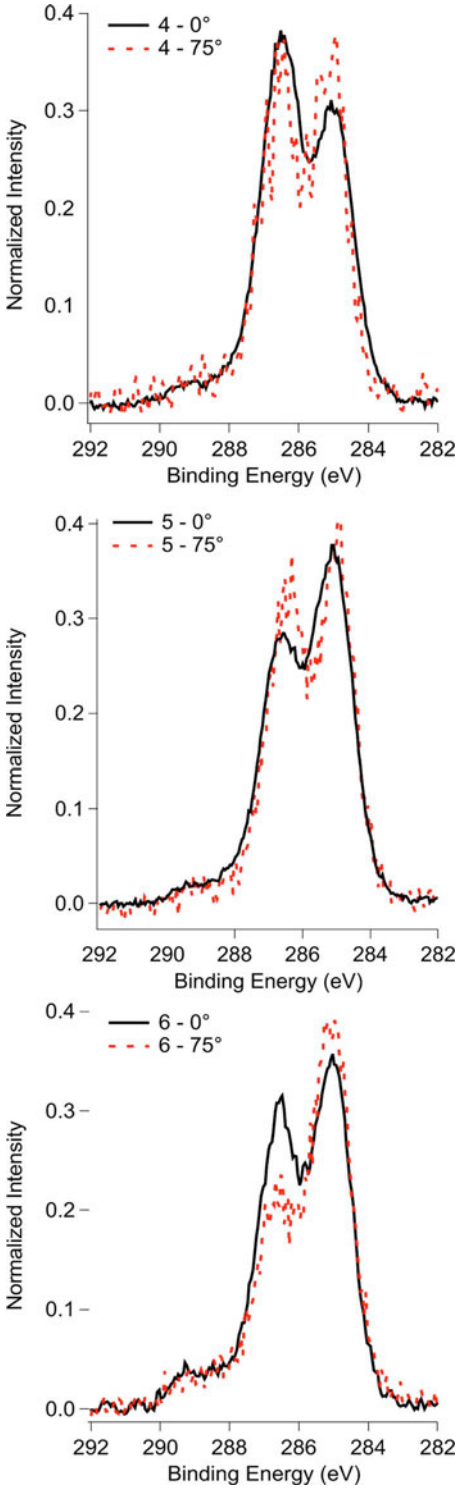

FIG. 2. XPS C 1*s* high resolution scans at 0° and 75° emission angles for (top) sample (4), (middle) sample (5), and (bottom) sample (6).

density profile extracted from x-ray reflectivity measurements are consistent with this hypothesis, as discussed later in the text.

B. X-ray reflectivity characterization of PEG-lipid surfaces

Reflectivity studies were carried out under ambient conditions to characterize the structure of OCT surfaces functionalized with PEG-lipid and PEG. The reflectivity graphs of all samples show at least two Kiessig fringes, indicating the formation of a well-defined film. Reflectivity data were plotted as R/q^{-4} to account for the Fresnel decay[36] and they were analyzed using the Parratt formalism.[33,37] Electron density profiles were modeled by boxes of different electron density, thickness, and roughness.

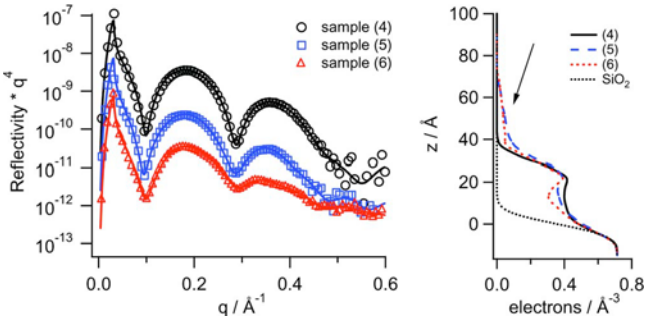

FIG. 3. (Left) X-ray reflectivity curves in air of samples (4), (5), and (6). Symbols represent experimental data and solid lines represent fits. (Right) Electron density profiles of samples (4), (5), and (6).

The reflectivity curves and corresponding electron density profiles for sample (4), prepared by the modification of a COOH-terminated alkylsilane film with PEG_{45}-lipid tethers, are shown in Fig. 3 with the reflectivity curves and corresponding electron density profiles for surfaces (5) and (6), which were obtained by the postfunctionalization of sample (4) with PEG_{17} and PEG_{45}, respectively. For reference, the profile of a bare silicon wafer with roughness of 0.47 nm has been superimposed on the electron density graph.

The film thickness, obtained from the electron density profiles, is roughly 3.5 nm for all surfaces. For a melt brush the most common measure of whether it is in the brush or mushroom regime is the ratio of brush thickness (z) to radius of gyration (Rg).[38] The radius of gyration of the polymer as formed in solution is estimated as $a(N/6)^{1/2}$ with a being the unit length of PEG_{45} (0.52 nm) and N the degree of polymerization (45). So for a PEG_{45} polymer Rg is equal to $0.52(45/6)^{1/2}=1.42$ nm. If we allow for the SAM (up to 0.8 nm) and the lipid tails (up to 1 nm) the PEG layer thickness is at least 1.7 nm and therefore: $z/Rg=1.7/1.42=1.2$. Since the brush regime corresponds to $z/Rg>1$ and the mushroom regime corresponds to $z/Rg<1$, these dry PEGLipid films are in an unextended brush regime.

It should be noted that the electron density profiles of samples (5) and (6), show an additional electron density tail separated more than 3.5 nm from the SiO_2 interface, which can be attributed to lipid tails phase separating from the PEG region, as indicated by the arrow in Fig. 3. The lack of such additional electron density in the profile of sample (4) indicates that in this case the lipid tails are embedded within the PEG region. These data clearly indicate that the backfilling of the PEG-lipid surface with PEG_{45} causes the lipid tails to be expelled to the region above the PEG layer, which is likely favorable for the formation of an elevated lipid membrane as discussed in the next section.

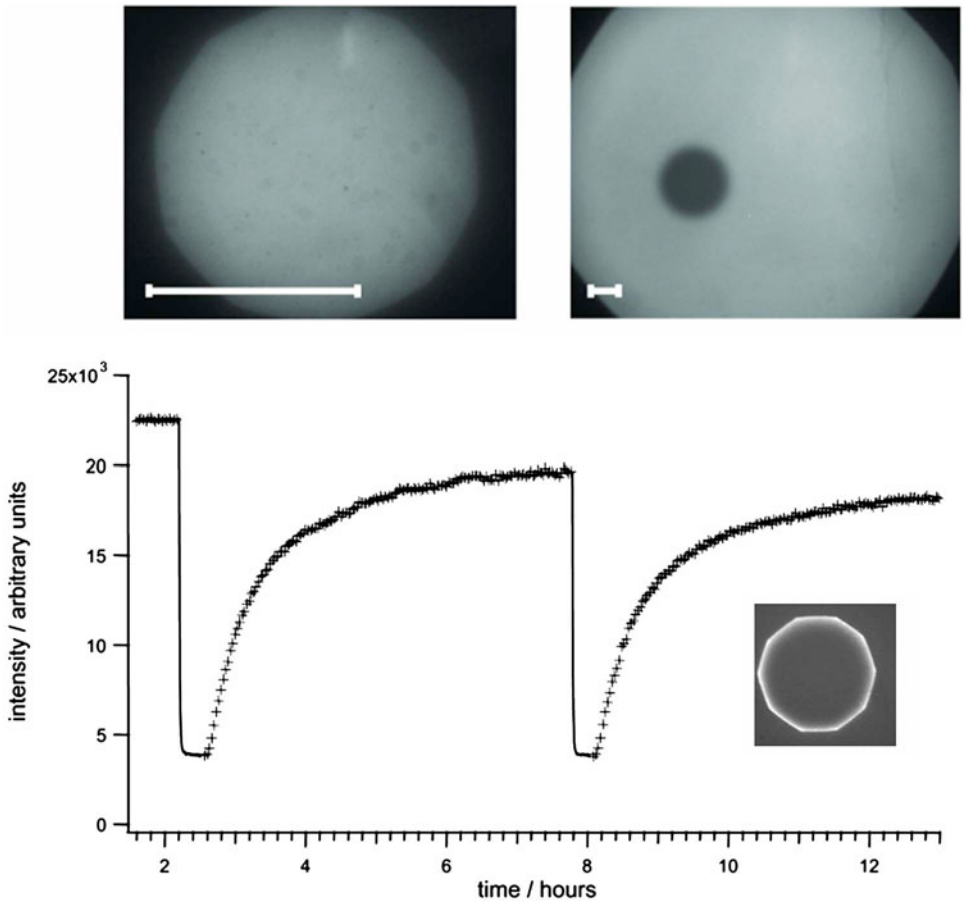

FIG. 4. (Top left) Fluorescence image showing homogeneous lipid membrane on representative backfilled sample (6) before bleaching (Objective 63×). (top right) Fluorescence image showing recovering bleached spot of lipid membrane on sample (6) (Objective 10×). Scale bar 25 μm. (bottom) Recovery profile for lipid membrane on sample (6), recorded in a central quadratic spot (4 μm^2) of the left image. Inset: Continuous bleaching results in the formation of a bright ring.

C. Fluorescence imaging of tethered lipid membranes

The formation of membranes was assessed by fluorescence microscopy after vesicle deposition on the PEGLipid surfaces. SOPC vesicles containing about 1 wt % of NBD labeled lipids were used for the fluorescence imaging. Continuous membranes formed on all samples and were found to be homogeneous across the entire sample area (about 1 cm^2); however, membrane formation occurred more readily on samples (5) and (6) than sample (4). This effect was likely due to the tether lipid tails becoming more available for membrane formation at the upper PEGLipid/air interface, as well as to improved density and homogeneity of the PEGLipid film after backfilling with PEG. A representative fluorescence image is shown in Fig. 4 (left). These membranes were found to be stable upon thorough washings and repeated drying/rehydrating cycles due to incorporation of PEG-lipid tethers within the membrane. It should be noted that deposition of SOPC vesicles on a PEG film, without PEG-lipid tethers, did not lead to formation of any membrane (data not shown). The membranes were also found to recover almost completely after fluorescence bleaching. To quantify the fluidity of the membrane, a sample spot with a diameter of about 100 μm was illuminated until complete bleaching of the dyes, as shown in Fig. 4 (right), and subsequent formation of a bright ring indicating fluidity of membrane components as shown in the inset of Fig. 4 (bottom). Then, the recovery of fluorescence intensity due to diffusion of unbleached lipids into the illuminated spot was followed as a function of time in the absence of continuous illumination. This was done to test whether the whole membrane was fluid or if it exhibited a substantial fraction of immobile lipids.

A SOPC membrane deposited on bare silicon oxide was investigated and used as a reference of a model fluid membrane[4] (data not shown). Both elevated membranes and silicon oxide supported membranes were found to be similarly fluid with recoveries above 90%, as shown in Fig. 4 (bottom). The corresponding diffusion constants calculated according to the continuous bleaching method[39] were found to be: 2.2 $\mu m^2\ s^{-1}$ for SOPC on SiO_2 and 2.1 $\mu m^2\ s^{-1}$ for membranes on samples (4), (5), and (6). These data compare well with previous reports, where diffusion constants were even correlated with height and mole percentage of tethers.[40,41] Some have also measured diffusion constants of tethered bilayers and of bilayers supported directly on silicon and have shown that comparable high diffusion constants

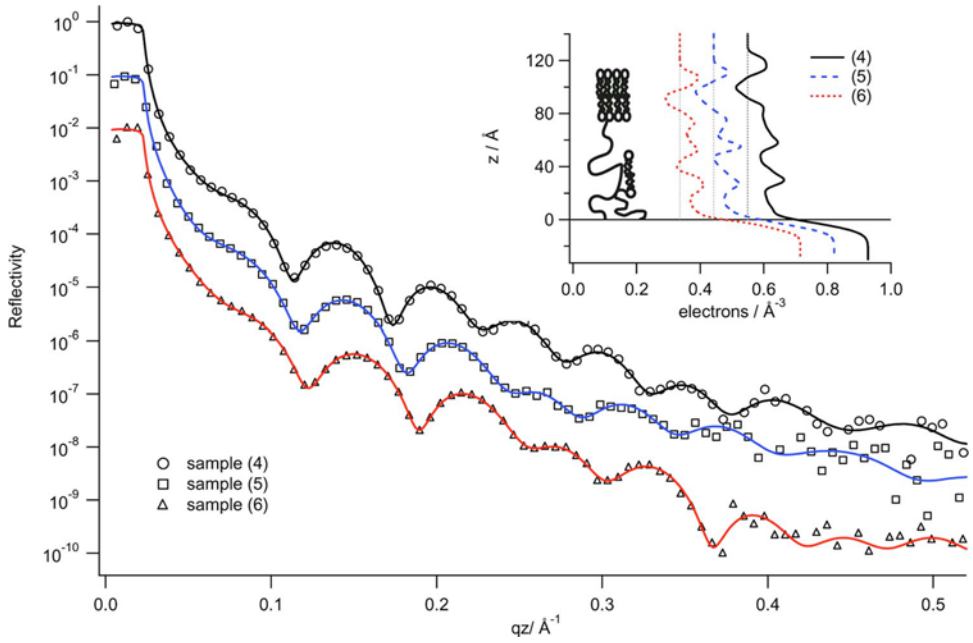

FIG. 5. (Left) X-ray reflectivity curve in water of lipid membrane deposited on samples (4), (5), and (6). (Right) Electron density profile of lipid membrane deposited on samples (4), (5), and (6). Curves for samples (5) and (6) are shifted for clarity.

have been obtained in both cases.[17] The somewhat higher absolute values of the diffusion constants measured here, i.e., a minor difference of ~2 versus ~1 $\mu m^2/s$, could be inherent to the different analyzing techniques. It is noteworthy that others have also measured higher diffusion constants for tethered membranes than they had expected before, showing a sensitive variation of the diffusivity of such "free-standing" membranes.[42] In summary, these fluorescence data prove the formation of fluid homogenous membranes supported on PEG-lipid films with diffusion constants and fluorescence recoveries similar to those of known silicon oxide supported bilayers.

D. X-ray reflectivity characterization of tethered lipid membranes

X-reflectivity was carried out in water at room temperature to characterize the structure of tethered lipid membranes after vesicle deposition on samples (4), (5), and (6). X-ray reflectivity curves and the corresponding electron density profiles are shown in Fig. 5.

All curves show seven Kiessig fringes as presented in Fig. 5 (left), indicating formation of well defined membranes. The solid lines represent a model fit based on assuming slabs of fixed thickness and roughness while varying the electron density to minimize chi.[2] The resulting electron density profiles together with a sketch representing the proposed cross section of the sample is shown in Fig. 5 (right). The region that is separated more than 12 nm from the Si wafer interface ($z=0$) represents the excess water [$\rho_e(H_2O)=0.334\ e^-/Å^3$]. The region between 8 and 12 nm from the Si surface shows the typical signature of a lipid bilayer; i.e., an increase above the density of water due to the topmost phosphate head groups of the lipids, a decrease below the density of water in the lipid alkyl region, and again an increase due to the headgroups of the lower leaflet. These three features indicate a lipid bilayer with a thickness of about 4 nm (Ref. 43) and show that the membrane is elevated above the surface by a distance of 8 nm in sample (4) and 7 nm in samples (5) and (6). Interestingly, a modified version of the bilayer signature also shows up in the region between 2 and 7 nm from the Si surface. However, the overall density in this region is higher than the density in the region between 8 and 12 nm. We suggest this region being interpreted as a coexistence of lipid micelles and PEG. Similar PEG-lipid micelle formation has been previously reported in the literature for a broad range of PEG-lipid molar concentration.[44,45] The region close to the interface ($z=0-2$ nm) exhibits a density, ρ_e, of about 400 e^-/nm^3, which is in good agreement with the presence of a PEG cushion of about 2 nm thickness.

The analysis of the x-ray data suggests that the uppermost bilayer is supported on a mixed phase composed of lipid micellular disks and fully extended PEG_{45}. This mixed phase is supported by a PEG cushion of 2 nm. The homogeneity of the fluorescence images suggests that the lateral size of the micelles is well below the optical limit. Also, the high recovery rate after photobleaching suggests that these micellular disks are fused to the uppermost bilayer, allowing for lipid transport from one phase to the other. This conclusion is in good agreement with the presence of two interconnected lipid regions like in hemifusion, the interconnection between lipid bilayers favored in the presence of PEG.[46] Alternatively, the mixed lipid/PEG phase may be a perforated lipid bilayer with pores being stabilized by the presence of PEG.

The major finding of this x-ray reflectivity study is the drastic elevation, about 7–8 nm, of the uppermost bilayer from the SiO_2 surface. Tamm and co-workers grafted a

PEG_{45}Lipid silane film to silicon oxide by Langmuir–Blodgett deposition and measured the swelling of the film after vesicle deposition by fluorescence interference-contrast microscopy. In contrast with our experiments, they used silicon chips with terraces of SiO_2 layers of different heights to gain nanometer scale resolution. They measured a distance of about 3.9 nm between the elevated membrane and the surface when the analysis was performed with four different heights of the terraces, but this value was reduced with 16 oxide heights due to capillary forces which are not present in our system. It is also possible that their preparation of the PEG-lipid film by Langmuir–Blodgett deposition prevented the formation of a mixed phase underneath the bilayer.

Experiments are currently in progress to gain a deeper insight into the structure underneath the elevated lipid bilayer. Shorter PEG chains are being used to check if the chain length and grafting density have an impact on micelle or pore formation. To better characterize this mixed lipid/PEG phase, we plan grazing incidence neutron scattering experiments, as well as neutron reflectometry experiments combined with contrast variation by deuteration of molecular components. Optical spectroscopic techniques like Förster resonance energy transfer could also prove very helpful in this approach.

IV. CONCLUSION

We have developed a novel, versatile architecture of a surface tethered lipid membrane with a variable distance from a silicon oxide surface in the 10 nm range. PEG-lipid tethers are first grafted to a self-assembled short-chain silane film and then additional PEG chains of variable length are introduced at the surface to provide better biological passivation of the substrate. XPS analysis near the C 1*s* ionization edge of dry PEG-lipid and mixed PEG-lipid/PEG films allowed us to confirm binding of PEG-lipid tethers to the silane film. Postfunctionalization with PEG caused lipid tails to stick up above the PEG layer, which was confirmed by the x-ray reflectometry measurements and turned out to be beneficial for membrane formation. X-ray reflectometry also showed that the thickness of PEG-lipid and mixed PEG-lipid/PEG films in air is about 3.5 nm.

Fluorescence imaging studies showed that membranes formed by vesicle fusion on PEG-lipid and mixed PEG-lipid/PEG films were homogeneous and fluid over the millimeter length scale. Stability of these membranes assessed by thorough washings and by drying/rehydrating cycles pointed to the incorporation of PEG-lipid tethers within the membrane. X-ray reflectivity studies showed that the tethered bilayers are elevated from the silicon oxide surface by about 8 nm. This large elevation height, well above the Flory radius of the tethers, is likely due to a layer composed of PEG and lipids underneath the elevated membrane. Our data interpretation for this submembrane region suggests a mixed phase comprising stretched PEG-lipid tethers, backfilled PEG, and lipids as micellular disks or bilayer patches. The novel two step procedure for functionalization of silicon dioxide surfaces, by tethering an elevated lipid bilayer and additionally passivating the underlying surface by soft hydrated polymers, provides an improved solid supported model cell membrane. Technically, this platform is very useful to easily form a high mobility elevated lipid bilayer by hydrating a dry film which is furthermore conveniently reusable even upon repeated drying/rehydrating cycles. Characteristics such as high membrane elevation and the presence of PEG, preventing protein nonspecific adsorption and denaturation on SiO_2, are promising for applications in protein studies, including membrane associated and transmembrane bulky proteins.

Finally, this approach to elevated tethered membranes bears potential as a tool for patterning membranes through chemically amplified constructive microlithography[47] where arrays of active esters can be used as templates for patterned membranes.

ACKNOWLEDGMENTS

The authors thank the EU for funding this work through the Marie Curie RTN network CIPSNAC (MRTN-CT-2003-504932). They also acknowledge financial support from BMBF (03RA6LMU). Funding was also provided by the NSF Graduate Research Fellowship (K.E.S.) and NSF DMR-Polymers Program under Grant No. 07-04539. This work made use of MRL Central Facilities supported by the MR-SEC Program of the National Science Foundation under Award No. DMR05-20415. The authors thank O. Seeck and R. L. Johnson for help with the D4 beamline at Hasylab, Hamburg and Kirstin Seidel and Christian Reich for help with reflectivity measurements.

[1]E. Sackmann, Science **271**, 43 (1996).
[2]L. Tamm and H. McConnell, Biophys. J. **47**, 105 (1985).
[3]A. L. Plant, Langmuir **9**, 2764 (1993).
[4]M. B. Hochrein, C. Reich, B. Krause, J. Rädler, and B. Nickel, Langmuir **22**, 538 (2006).
[5]R. P. Richter, J. Lai Kee Him, B. Tessier, C. Tessier, and A. R. Brisson, Biophys. J. **89**, 3372 (2005).
[6]B. W. Koenig, S. Krueger, W. J. Orts, C. F. Majkrzak, N. F. Berk, J. Silverton, and K. Gawrisch, Langmuir **12**, 1343 (1996).
[7]A. Lambacher and P. Fromherz, J. Opt. Soc. Am. B **19**, 1435 (2002).
[8]E. Sackmann and R. Bruinsma, ChemPhysChem **3**, 262 (2002).
[9]E. Sackmann and M. Tanaka, Trends Biotechnol. **18**, 58 (2000).
[10]J. Radler and E. Sackmann, Curr. Opin. Solid State Mater. Sci. **2**, 330 (1997).
[11]P. Theato and R. Zentel, Langmuir **16**, 1801 (2000).
[12]J. Y. Wong, J. Majewski, M. Seitz, C. K. Park, J. N. Israelachvili, and G. S. Smith, Biophys. J. **77**, 1445 (1999).
[13]M. Kühner and E. Sackmann, Langmuir **12**, 4866 (1996).
[14]M. Schaub, G. Wenz, G. Wegner, A. Stein, and D. Klemm, Adv. Mater. **5**, 919 (1993).
[15]C. Dietrich and R. Tampe, Biochim. Biophys. Acta **1238**, 183 (1995).
[16]F. Albertorio, A. J. Diaz, T. Yang, V. A. Chapa, S. Kataoka, E. T. Castellana, and P. S. Cremer, Langmuir **21**, 7476 (2005).
[17]M. L. Wagner and L. K. Tamm, Biophys. J. **79**, 1400 (2000).
[18]C. Delajon, T. Gutberlet, R. Steitz, H. Möhwald, and R. Krastev, Langmuir **21**, 8509 (2005).
[19]A. M. Pilbat, Z. Szegletes, Z. Kota, V. Ball, P. Schaaf, J. C. Voegel, and B. Szalontai, Langmuir **23**, 8236 (2007).
[20]R. J. Merath and U. Seifert, Phys. Rev. E **73**, 010401 (2006).
[21]M. Seitz, E. Ter-Ovanesyan, M. Hausch, C. Park, J. A. Zasadzinski, R. Zentel, and J. N. Israelachvili, Langmuir **16**, 6067 (2000).
[22]D. J. McGillivray, G. Valincius, D. J. Vanderah, W. Febo-Ayala, J. T. Woodward, F. Heinrich, J. J. Kasianowicz, and M. Lösche, Biointerphases **2**, 21 (2007).

[23]V. Kiessling and L. K. Tamm, Biophys. J. **84**, 408 (2003).
[24]O. Purrucker, A. Förtig, R. Jordan, and M. Tanaka, ChemPhysChem **5**, 327 (2004).
[25]V. Atanasov, N. Knorr, R. S. Duran, S. Ingebrandt, A. Offenhäusser, W. Knoll, and I. Köper, Biophys. J. **89**, 1780 (2005).
[26]W. W. Shen, S. G. Boxer, W. Knoll, and C. W. Frank, Biomacromolecules **2**, 70 (2001).
[27]N. Bunjes, E. K. Schmidt, A. Jonczyk, F. Rippmann, D. Beyer, H. Ringsdorf, P. Gräber, W. Knoll, and R. Naumann, Langmuir **13**, 6188 (1997).
[28]D. Schwendel, R. Dahint, S. Herrwerth, M. Schloerholz, W. Eck, and M. Grunze, Langmuir **17**, 5717 (2001).
[29]S. Tokumitsu, A. Liebich, S. Herrwerth, W. Eck, M. Himmelhaus, and M. Grunze, Langmuir **18**, 8862 (2002).
[30]S. R. Wasserman, Y. T. Tao, and G. M. Whitesides, Langmuir **5**, 1074 (1989).
[31]J. Li and J. H. Horton, J. Mater. Chem. **12**, 1268 (2002).
[32]C. Reich, M. Hochrein, B. Krause, and B. Nickel, Rev. Sci. Instrum. **76**, 095103 (2005).
[33]L. G. Parratt, Phys. Rev. **95**, 359 (1954).
[34]P. S. Pershan, Phys. Rev. E **50**, 2369 (1994).
[35]A. Williams and I. T. Ibrahim, Chem. Rev. **81**, 589 (1981).
[36]G. T. Hermanson, *Bioconjugate Techniques* (Academic, New York, 1996), pp. 139–140.
[37]H. Kiessig, Ann. Phys. **402**, 769 (1931).
[38]L. Andruzzi, A. Hexemer, X. Li, C. K. Ober, E. J. Kramer, G. Galli, E. Chiellini, and D. A. Fischer, Langmuir **20**, 10498 (2004).
[39]C. Dietrich, R. Merkel, and R. Tampe, Biophys. J. **72**, 1701 (1997).
[40]M. A. Deverall, E. Gindl, E. K. Sinner, H. Besir, J. Ruehe, M. J. Saxton, and C. A. Naumann, Biophys. J. **88**, 1875 (2005).
[41]P. F. F. Almeida, W. L. C. Vaz, and T. E. Thompson, Biochemistry **31**, 7198 (1992).
[42]C. A. Naumann, O. Prucker, T. Lehmann, J. Rühe, W. Knoll, and C. W. Frank, Biomacromolecules **3**, 27 (2002).
[43]J. F. Nagle and S. Tristam-Nagle, Biochim. Biophys. Acta **1469**, 159 (2000).
[44]D. Marsh, R. Bartucci, and L. Sportelli, Biochim. Biophys. Acta **1615**, 33 (2003).
[45]S. Belsito, R. Bartucci, G. Montesano, D. Marsh, and L. Sportelli, Biophys. J. **78**, 1420 (2000).
[46]R. N. Orth, J. Kameoka, W. R. Zipfel, B. Ilic, W. W. Webb, T. G. Clark, and H. G. Craighead, Biophys. J. **85**, 3066 (2003).
[47]L. Andruzzi, B. Nickel, G. Schwake, J. O. Rädler, K. E. Sohn, T. E. Mates, and E. J. Kramer, Surf. Sci. (in press).
[48]See EPAPS Document No. E-BJIOBN-2-003703 for a sketch of the set up used to perform x-ray reflectometry and fluorescence measurements on a hydrated lipid membrane. This document can be reached through a direct link in the online article's HTML reference section or via the EPAPS homepage (http://www.aip.org/pubservs/epaps.html).